34th Annual International Conference of the IEEE EMBS
San Diego, California USA, 28 August - 1 September, 2012

Arrhythmogenic substrate for atrial fibrillation: Insights from an integrative computational model of pulmonary veins

Oleg V. Aslanidi*, Michael A. Colman*, Jichao Zhao, Bruce H. Smaill,
Stephen H. Gilbert, Jules C. Hancox, Mark R. Boyett, Henggui Zhang

Abstract—**Mechanisms underlying the genesis of re-entrant substrate for atrial fibrillation (AF) in the pulmonary veins (PVs) and left atrium (LA) are not well understood. We develop a biophysically detailed computational model for the PVs and surrounding LA tissue. The model integrates canine PV and LA single cell electrophysiology with the respective 3D tissue geometry and fiber orientation reconstructed from micro-CT data. The model simulations demonstrate that a combination of tissue anisotropy and electrical heterogeneity between the PVs and LA causes a break-down of normal electrical excitation wave-fronts. This leads to the generation of a high-frequency re-entrant source near the PV sleeves. Evidence of such sources have been seen clinically in AF patients. In summary, our modeling results provide new insights into the arrhythmogenic mechanisms of re-entrant excitation waves underlying AF.**

I. Introduction

Atrial fibrillation (AF), associated with irregular electrical activation of the atria, is the most common sustained cardiac arrhythmia [1]. The rate of hospitalization for AF and costs of its treatment are increasing in epidemic proportions [2]. AF is a major cause of morbidity and mortality, resulting in a reduction in cardiac output, predisposition to heart failure and stroke, and increased sudden death rates [1, 2]. However, mechanisms underlying the genesis of AF are incompletely understood and its clinical treatments all have significant intrinsic limitations.

The myocardial sleeves of the pulmonary veins (PVs) in the left atrium (LA) are recognized as main sources of high-frequency electrical activity during AF, and the PV ablation is widely used to terminate AF [3]. Ex-vivo studies of the PV sleeves have demonstrated repolarization heterogeneities and complex anisotropic arrangement of fibers, which result in conduction blocks and signs of incomplete re-entry [3-5]. Similar activation patterns have been observed at the PV-LA junctions during catheter mapping in AF patients, which led to suggestions that high-frequency activity in the PV can be sustained by re-entry [6]. However, mechanisms by which interactions of the electrical heterogeneity and conduction anisotropy in the PVs can generate arrhythmic substrate are difficult to dissect in experimental or clinical settings.

Computational modeling provides an efficient framework for integrating multi-scale and multi-modal biophysical data and understanding arrhythmogenesis in the 3D atria [7-10]. Electrophysiological models for the canine LA and PV cells have been developed recently [11]. However, structural complexity makes it difficult to quantify fine 3D details of the PV structure, such as fiber orientation. Thus, even the most recent 3D models of atrial activation have not included descriptions of the PV anatomy and electrophysiology [10].

The aim of this paper is primarily to develop and study an integrative biophysically detailed 3D model of the canine PVs and surrounding LA tissue. The details of tissue geometry and fiber orientation are based on a recent micro-CT reconstruction of the 3D canine atria [12]. The model is used to explore the role of electrical heterogeneity and fiber anisotropy in the genesis of re-entrant waves in the atria.

II. Methods

A. Model Development

The dynamics of electrical excitation in atrial tissues can be described by the following well-known equation [7-10]:

$$\frac{\partial V}{\partial t} = \nabla \cdot \mathrm{D} \nabla V - \frac{I_{\mathrm{ion}}}{C_m} \,. \qquad (1)$$

Here V (mV) is the membrane voltage, ∇ is a spatial gradient operator, t is time (s), D is a diffusion coefficient ($\mathrm{mm}^2\ \mathrm{ms}^{-1}$) that characterizes electrotonic spread of voltage via gap junctional coupling, I_{ion} is the total membrane ionic current (pA), and C_{m} (pF) is the membrane capacitance.

Biophysically detailed models for individual ionic channel currents (such as I_{CaL}, I_{to}, I_{Kr}, I_{Ks}, I_{K1}) that comprise I_{ion} have been developed for the canine LA and PV cells [11]. The models accurately reproduce the voltage-clamp data on which it has been based, and provide feasible morphologies for the action potential (AP) in these distinctive cell types.

Manuscript submitted June 1, 2012. This work was supported by a project grant from the British Heart Foundation (PG/10/69/28524), United Kingdom.

O. V. A. Author is with the Division of Imaging Sciences & Biomedical Engineering, King's College London, London SE1 7EH, United Kingdom (tel: +44-20-718-87188; e-mail: oleg.aslanidi@kcl.ac.uk).

M. A. C. and H. Z. Authors are with the School of Physics and Astronomy, University of Manchester, Manchester M13 9PL, United Kingdom (e-mails: michael.colman@postgrad.manchester.ac.uk and henggui.zhang@manchester.ac.uk, respectively).

J. Z. and B. H. S. Authors are with Auckland Bioengineering Institute, University of Auckland, Auckland 1010, New Zealand (e-mails: j.zhao@auckland.ac.nz and b.smaill@auckland.ac.nz, respectively).

S. H. G. Author is with the Institute of Membrane & Systems Biology, University of Leeds, Leeds LS2 9JT, United Kingdom (email: s.h.gilbert@leeds.ac.uk).

J. C. H. Author is with the School of Physiology & Pharmacology, University of Bristol, Bristol BS8 1TD, United Kingdom (email: jules.hancox@bristol.ac.uk).

M. R. B. Author is with the Faculty of Medical & Human Sciences, University of Manchester, Manchester M13 9NT, United Kingdom (e-mail: mark.boyett@manchester.ac.uk).

*O. V. A. and M. A. C. equally contributed to this work.

A novel method of contrast micro-CT has been applied recently [12] to reconstruct the detailed 3D geometry of the canine atria and segment it into distinctive regions, including PVs. Structure tensor analysis validated by histology has shown that the arrangement of atrial fibers can be quantified using the micro-CT images, as the contrast agent (iodine) preferentially accumulates within the myocardiac fibers. Hence, fiber orientation in the atrial bundles, including PV sleeves, has been reconstructed [12]. Fig. 1 illustrates the 3D geometry (Fig. 1A) and fiber orientation (Fig. 1B) in the PVs and surrounding atrial tissue, along with the cellular APs.

B. Model simulations

Eq. (1) was used to simulate AP propagation in the 3D model integrating the cellular electrophysiology with tissue geometry and fiber orientation. The diffusion coefficients in the longitudinal and transverse fiber directions were set to the values 0.10 mm^2 ms^{-1} and 0.01 mm^2 ms^{-1}, respectively [10]. Eq. (1) was solved using the explicit Euler method with time and space steps $\Delta t = 0.005$ ms and $\Delta x = 0.2$ mm.

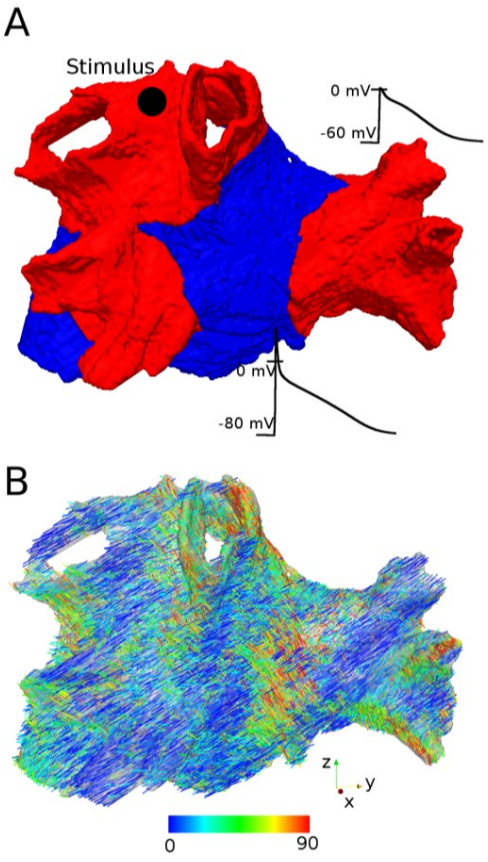

Fig. 1. 3D model of the canine PVs. A: Segmented geometry of two pairs of branching PVs (red) and surrounding LA tissue (blue). Single cell APs for the PV and LA regions are shown. Black dot corresponds to the pacing site used in all simulations. B: Fiber orientation, with the fibers colored according to their inclination angle ("rainbow" palette). Most fibers are aligned along the PVs, but their arrangement becomes more complex - with multiple changing directions - towards the LA, which is in agreement with electro-anatomical studies [4].

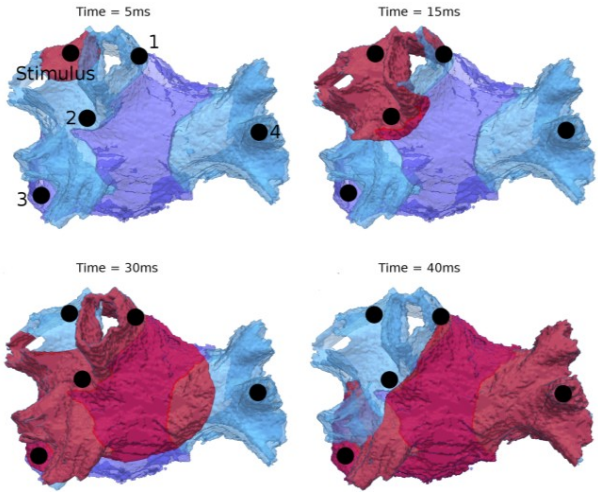

Fig. 2. Regular excitation wave propagation following S1 stimulus. Here and in the following figures, the PV and LA tissue geometries are shown in transparent light and dark blue colors, respectively. Snapshots of the membrane potential wave are shown as iso-surfaces at V = -30 mV (dark red) for 4 successive moments of time. Black dots 1-4 mark several key "recording" sites similar to positions of electrodes in electrophysiological tissue experiments [14].

The roles of tissue heterogeneity and anisotropy were investigated as follows. Under normal conditions the tissue was segmented into the PV and LA regions, with different cell-specific AP models used in each region (Fig. 1A). The role of heterogeneity was studied by using the PV model only throughout the entire tissue. The role of anisotropy was studied by setting the anisotropy ratio for conduction along and transverse to the fibers to1:1 instead of the normal 10:1.

The same pacing protocol was used in all simulations. Electrical stimuli were applied to a region within the PV with abruptly changing directions of anisotropic fibers, as such areas have been shown to be prone to conduction blocks [4]. Two S1 stimuli were applied at a cycle length of 120 ms, followed by a short-coupled "ectopic" S2 stimulus at 90 ms.

III. RESULTS

Fig. 2 shows propagation of a regular excitation wave-front initiated by S1 stimulation in the PV region. After the initiation, the wave propagates through the pair of nearby PVs and exits into the LA via points 1 and 2 at ~15 ms, and then via point 3 at 30 ms (Fig 2). The wave then propagates throughout the LA tissue and enters the second pair of PVs at the opposite side of the LA; point 4 is reached at 40 ms.

Application of a short-coupled "ectopic" S2 stimulus resulted in a break-down of the regular excitation wave-front and generation of a re-entrant wave (Fig. 3). Note that conduction of the wave initiated by the S2 stimulus was slowed down as the tissue has not fully recovered from the previous S1 stimulation (S1-S2 coupling interval of 90 ms was significantly lower than the AP duration of ~120 ms). Hence, whereas the waves initiated by the S1 stimulus propagated into the LA via points 1 and 2 at ~15 ms (Fig. 2),

the wave initiated by the S2 stimulus failed to propagate into the LA via same points 1 and 2, as the LA tissue has not fully repolarized even at 20 ms (Fig 3). Instead, the wave entered the LA via point 3 at 45 ms, by which time the entire LA has repolarised. Therefore, the wave spread throughout the LA in multiple directions at 55-65 ms (Fig. 3). The wave was blocked from re-entering the PV at point 2 at ~55 ms. However, after ~85 ms of slow propagation through the superior part of the LA, the wave reached the PV at point 1 and propagated towards the initial stimulation point (Fig. 3). Hence, the full re-entrant circuit has been completed.

We have previously shown that the AP heterogeneity plays a role in the initiation of re-entrant waves, whereas anisotropy can cause irregular, multiple re-entrant circuits in the right atrium [9, 10]. Therefore, we studied the role of tissue electrical heterogeneity and anisotropy in the PV-LA. Fig. 4 shows wave propagation patterns for two cases (see Methods): the model with anisotropy but no heterogeneity (Fig. 4A), and the model with AP heterogeneity but no anisotropy (Fig. 4B). The same S2 "ectopic" stimulus was applied as in the full model illustrated in Fig. 3.

Fig. 4A shows that due to the removal of AP heterogeneity between the PV and LA, there is no longer conduction block towards the LA. Hence, a regular excitation wave-front propagates throughout the tissue (Fig. 4A), similar to that seen after the S1 stimulation in Fig. 2. As shown in Fig. 4B, the initial conduction block towards the LA is present due to the AP heterogeneity. However, the absence of anisotropy (primarily, fast and slow conducting pathways) results in the elimination of the re-entrant circuit (Fig. 4B).

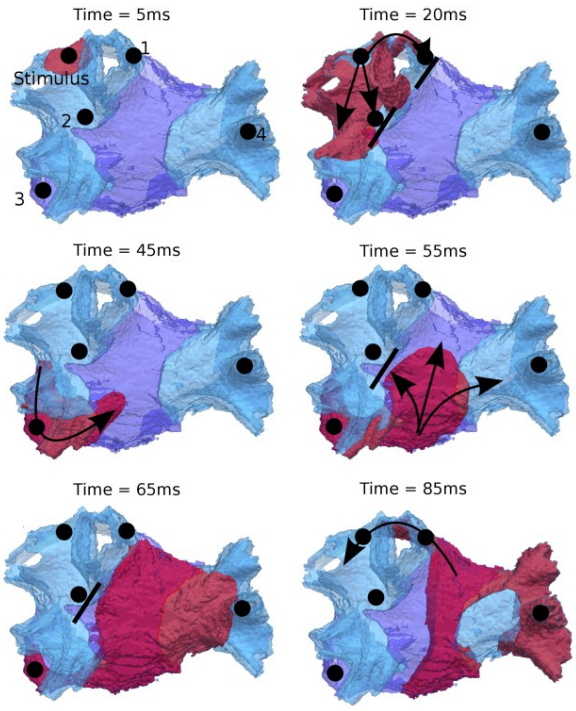

Fig. 3. Re-entrant wave propagation following "ectopic" S2 stimulus. Colors as in Fig. 2. Black arrows show direction of wave-front propagation and black lines mark areas of the conduction block.

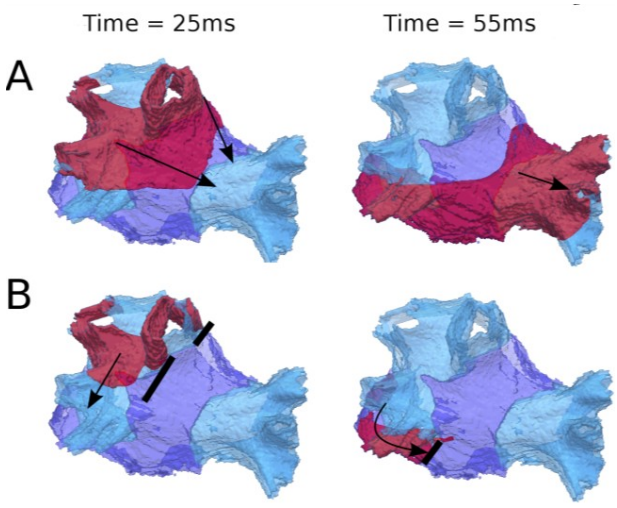

Fig. 4. The role of tissue heterogeneity and anisotropy in re-entry initiation and sustenance. A: regular wave-front propagation following "ectopic" S2 stimulus in the homogeneous tissue. B: initial conduction block does not lead to re-entry in the isotropic tissue.

IV. DISCUSSION

We developed a detailed 3D computational model (Fig. 1) that integrated the PV and LA single cell electrophysiology [11] with the respective 3D tissue geometry and fiber orientation reconstructed from contrast micro-CT data [12]. The model simulations demonstrated (Figs. 2-4) that a combination of tissue anisotropy and electrical heterogeneity at the PV sleeves caused a break-down of the regular electrical excitation wave-fronts leading to the generation of a high-frequency re-entrant source near the PVs (Fig. 5).

Experimental ex-vivo studies have previously shown that the PV sleeves can provide a substrate for the AP conduction block and re-entry [4, 5, 14]. Evidence of such re-entrant sources have also been seen clinically in AF patients [3, 6]. Our computational study for the first time dissected both the pattern (Fig. 3) and mechanisms (Fig. 4) of such re-entry initiation. Note that some effects of tissue substrates on the atrial conduction have been simulated previously [7, 8], but heterogeneity and anisotropy in these studies were not based on relevant data. Results of the present modeling study provide new quantitative insights into the arrhythmogenic mechanisms of re-entrant excitation waves underlying AF.

Models of the atria have been largely based on tissue geometries reconstructed from histological data [7, 10, 15]. While these models included many details of atrial anatomy, their segmentation into distinctive tissue sub-domains was either absent [15] or based on phenomenological estimations of the sub-domain locations [7]. Moreover, even the most biophysically detailed 3D models [10] have not included electrophysiology and fiber architecture in the PV sleeves, which are crucial in the genesis of AF [3-6]. Therefore, the 3D model presented in this study provides a missing link to the computational modeling of the atria and AF. In future, the PV model developed in this study will be added to larger

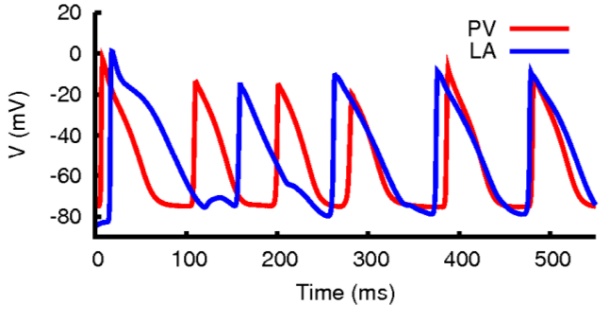

Fig. 5. Sustenance of re-entry initiated in the PVs. Periodic APs recorded from the PV and LA regions during the onset of re-entry (shown in Fig. 3), and its further progression over several periods.

scale models of the entire 3D atria [10, 12] and used for dissecting the global mechanisms of AF arrhythmogenesis.

Future detailed atrial modeling must take into account (i) differential anisotropy ratios in various parts of the atria (which can vary from ~9:1 to 36:1 in the PV region alone, with the high-anisotropy areas sustaining micro re-entry [4]), (ii) detailed variability of cell electrophysiology parameters, such as the densities of ionic currents (I_{CaL}, I_{K1}, I_{Ks}) that determine the AP duration [10, 11], (iii) conditions affecting atrial conduction, such as pathological changes in the ionic channel densities and vagal tone [16, 17], (iv) effective size of the tissue substrate which determines the extent of re-entry meandering [16, 18]. After such a stratification, followed by validation against detailed atrial mapping data [19, 20], the models may not only explain the qualitative mechanisms of AF, but also give quantitative insights into pharmacological modulation and prevention of the disease [21, 22].

REFERENCES

[1] D. Dobrev, and S. Nattel. "New insights into the molecular basis of atrial fibrillation: mechanistic and therapeutic implications." *Cardiovasc. Res.*, vol. 89, pp. 689-691, 2011.

[2] E. Anter, M. Jessup, and D.J. Callans. "Atrial fibrillation and heart failure: treatment considerations for a dual epidemic." *Circulation*, vol. 119, pp. 2516-2525, 2009.

[3] M. Haissaguerre, P. Jais, D.C. Shah, et al. "Spontaneous initiation of atrial fibrillation by ectopic beats originating in the pulmonary veins." *N. Engl. J. Med.*, vol. 339, pp. 659-666, 1998.

[4] M. Hocini, S.Y. Ho, T. Kawara, et al. "Electrical conduction in canine pulmonary veins: electrophysiological and anatomic correlation." *Circulation*, vol. 105, pp. 2442-2448, 2002.

[5] R. Arora, S. Verheule, L. Scott, et al. "Arrhythmogenic substrate of the pulmonary veins assessed by high-resolution optical mapping." *Circulation*, vol. 107, pp. 1816-1821, 2003.

[6] K. Kumagai, M. Ogawa, H. Noguchi, T. Yasuda, H. Nakashima, and K. Saku. "Electrophysiologic properties of pulmonary veins assessed using a multielectrode basket catheter." *J. Am. Coll. Cardiol.*, vol. 43, pp. 2281-2289, 2004.

[7] G. Seemann, C. Hoper, F.B. Sachse, O. Dossel, A.V. Holden, and H. Zhang. "Heterogeneous three-dimensional anatomical and electrophysiological model of human atria." *Phil. Trans. Roy. Soc. A*, vol. 364, pp. 1465-1481, 2006.

[8] M. Ridler, D.M. McQueen, C.S. Peskin, and E. Vigmond. "Action potential duration gradient protects the right atrium from fibrillating." In *Conf. Proc. 2006 IEEE Eng. Med. Biol. Soc.*, pp. 3978-3981.

[9] O.V. Aslanidi, M.R. Boyett, H. Dobrzynski, J. Li, and H. Zhang. "Mechanisms of transition from normal to reentrant electrical activity in a model of rabbit atrial tissue: interaction of tissue heterogeneity and anisotropy." *Biophys. J.*, vol. 96, pp. 798-817, 2009.

[10] O.V. Aslanidi, M.A. Colman, J. Stott, H. Dobrzynski, M.R. Boyett, A.V. Holden, and H. Zhang. "3D virtual human atria: a computational platform for studying clinical atrial fibrillation." *Prog. Biophys. Mol. Biol.*, vol. 107, pp. 156-168, 2011.

[11] O.V. Aslanidi, T.D. Butters, C.X. Ren, G. Ryecroft, and H. Zhang. "Electrophysiological models for the heterogeneous canine atria: computational platform for studying rapid atrial arrhythmias." In *Conf. Proc. 2011 IEEE Eng. Med. Biol. Soc.*, pp. 1693-1696.

[12] O.V. Aslanidi, T. Nikolaidou, J. Zhao, et al. Application of X-Ray micro-computed tomography with iodine staining to cardiac imaging, segmentation and computational model development. *IEEE Trans. Med. Imaging*, under review.

[13] M.S. Spach, P.C. Dolber, and J.F. Heidlage. "Interaction of inhomogeneities of repolarization with anisotropic propagation in dog atria: a mechanism for both preventing and initiating reentry." *Circ. Res.*, vol. 65, pp. 1612-1631, 1989.

[14] S.-L. Chang, Y.-C. Chen, Y.-H. Yeh, et al. "Heart failure enhances arrhythmogenesis in pulmonary veins." *Clin. Exp. Pharmacol. Physiol.*, vol. 38, pp. 666-674, 2011.

[15] E.M. Cherry, and S.J. Evans. "Properties of two human atrial cell models in tissue: restitution, memory, propagation, and reentry." *J. Theor. Biol.*, vol. 254, pp. 674-690, 2008.

[16] S.V. Pandit, O. Berenfeld, J.M. Anumonwo, R.M. Zaritski, J. Kneller, S. Nattel, and J. Jalife. "Ionic determinants of functional reentry in a 2-D model of human atrial cells during simulated chronic atrial fibrillation." *Biophys. J.*, vol. 88, pp. 3806-3821, 2005.

[17] T.D. Butters, O.V. Aslanidi, S. Inada, M.R. Boyett, J.C. Hancox, M. Lei, and H. Zhang. "Mechanistic links between Na^+ channel (SCN5A) mutations and impaired cardiac pacemaking in sick sinus syndrome." *Circ. Res.*, vol. 107, pp. 126-137, 2010.

[18] O.V. Aslanidi, A. Bailey, V.N. Biktashev, R.H. Clayton, and A.V. Holden. "Enhanced self-termination of re-entrant arrhythmias as a pharmacological strategy for antiarrhythmic action." *Chaos*, vol. 12, pp. 843-851, 2002.

[19] H. Hayashi, R.L. Lux, R.F. Wyatt, M.J. Burgess, and J.A. Abildskov. "Relation of canine atrial activation sequence to anatomic landmarks." *Am. J. Physiol.*, vol. 242, pp. H421-428, 1982.

[20] S. Sakamoto, T. Nitta, Y. Ishii, Y. Miyagi, H. Ohmori, and K. Shimizu. "Interatrial electrical connections: the precise location and preferential conduction. *J. Cardiovasc. Electrophysiol.*, vol. 16, pp. 1077-1086, 2005.

[21] O.V. Aslanidi, M. Al-Owais, A.P. Benson, et al. "Virtual tissue engineering of the human atrium: Modelling pharmacological actions on atrial arrhythmogenesis." *Eur. J. Pharm. Sci.*, vol. 46, pp. 209-221, 2012.

[22] T. Datino, L. Macle, D. Chartier, P. Comtois, P. Khairy, P.G. Guerra, F. Fernandez-Aviles, and S. Nattel. Differential effectiveness of pharmacological strategies to reveal dormant pulmonary vein conduction: a clinical-experimental correlation. *Heart Rhythm*, vol. 8, pp. 1426-1433, 2011.